Modeling of Bright Band Having a Smooth Connection to Snowfall for Observation of Rain from Space

Jun AWAKA [1], Nobuhiro TAKAHASHI [2], Toshio IGUCHI [2]
[1] *Department of Information Science, Hokkaido Tokai University*
Minami-ku, Minami-sawa 5-1-1-1, Sapporo 005-8601, Japan, awaka@de.htokai.ac.jp
[2] *NiCT (National Institute of Information and Communications Technology)*
4-2-1 Nukui-kita-machi, Koganei, Tokyo184-8795, Japan

Abstract

This paper proposes a bright band (BB) model in which the radar reflectivity factor (Z) shows a reasonable connection to that in the upper snow region. The model assumes a linear change of precipitation rate with hight and also a linear change in slope of drop-size distribution with height in the upper part of BB. A comparison of the model with an averaged height profile of Z obtained by the TRMM precipitation radar shows a good agreement.

1. INTRODUCTION

In radar observation of rain from space, such as in the case of the Tropical Rainfall Measuring Mission (TRMM) [1], information about the bright band (BB) becomes very important for a successful retrieval of rainfall rate because the radar signal passes through the bright band which causes appreciable attenuation.

Literatures [2][3] show that the precipitation rate of snow, which may exist above BB, is at most a few mm/h whereas the precipitation rate of rain which accompanies BB is much higher and sometimes can be larger than 10 mm/h. Unfortunately, however, existing BB models do not seem to explain the difference between the small precipitation rate of snow above BB and the large precipitation rate in the lower part of BB. This paper tries to develop a model which can handle the change of precipitation rate in height from upper snow region to rain region with BB in between.

2. DESCRIPTION OF THE MODEL

We adopt the model by Sekhon and Srivastava [3] as the basic model for snowfall: The fall velocity of a snowflake, v_s [cm/s] is assumed to be

$$v_s(D) \;=\; 207D^{0.31} \tag{1}$$

where D is the melted diameter in [cm]. The drop size distribution (DSD) of snowflakes, $N_s(D)$, is assumed to be expressed by

$$N_s(D) \;=\; N_{os}\exp(-\Lambda D) \qquad [\mathrm{mm^{-1}m^{-3}}] \tag{2}$$

with

$$\Lambda \;=\; 22.9R^{-0.45} \qquad [\mathrm{cm^{-1}}] \tag{3}$$

where R [mm/h] is the precipitation rate.

The maximum diameter of the melted particle is assumed to be $D_{max} = 7$ mm, which is the same as the maximum diameter of raindrop, and is regarded as a constant, meaning that D_{max} does not change with height. Then, Eq.(3) alone uniquely determines $N_s(D)$ because N_{os} in (2) is automatically determined in such a way that R in (3) is consistent with the precipitation rate which is calculated from (1) and (2), that is

$$R = \int_0^{D_{max}} \frac{4\pi}{3}\Big(\frac{D}{2}\Big)^3 v_s(D)N_s(D)dD \times 10^{-4} \times 3600 \tag{4}$$

Since (4) is expressed in terms of melted diameter, (4) also holds in the case of BB and rain when the subscript $_s$ is dropped from v_s and N_s.

The melted mass fraction, F, in BB is numerically computed by integrating a heat budget equation described in Yokoyama and Tanaka [4] by using the fall velocity of a snowflake computed by (1) and the fall velocity of a raindrop v_R [cm/s] computed by the formula given in Foote and Du Toit [5].

When F is obtained, the volume water content, P_w, and the density, ρ_B [g/cm^3], of a particle in BB is shown to be given as follows:

$$P_w \;=\; \frac{F}{F + \frac{\rho_w}{\rho_{s0}}(1-F)} \tag{5}$$

$$\rho_B \;=\; \frac{\rho_w}{F + \frac{\rho_w}{\rho_{s0}}(1-F)} \tag{6}$$

where ρ_w [g/cm^3] is the density of water, and ρ_{s0} [g/cm^3] is the density of snow at the top of BB where $F = 0$.

The fall velocity of a particle in BB, v_B [cm/s], is

$$v_B(D) \;=\; v_R(D)\Big(\frac{\rho_B}{\rho_w}\Big)^{1/3}\sqrt{\frac{X}{1+(X-1)F}} \tag{7}$$

where

$$X \;=\; \Big(\frac{v_{s0}}{v_R}\Big)^2\Big(\frac{\rho_w}{\rho_{s0}}\Big)^{2/3} \tag{8}$$

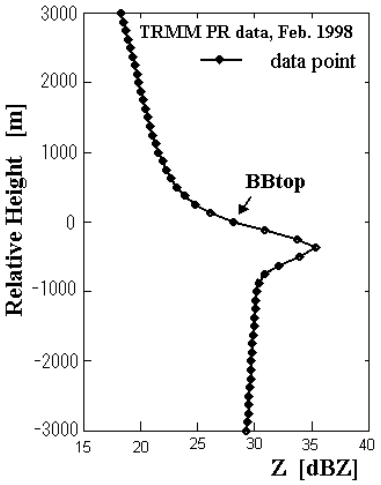

Fig. 1: Averaged profile of BB observed by TRMM PR The height is measured relative to the height of BBtop.

The above (7) and (8) are obtained by assuming that the drag coefficient of a BB particle is a linear function of F [4].

We assume that the BB particle is a uniform mixture of water, ice, and air. In this study, we use Nishitsuji model [6][7][8]. (For other uniform mixture models, see e.g. [9].)

In the Nishitsuji model, the dielectric constant of BB particle is calculated by the following Wiener's formula

$$\frac{\epsilon_B - 1}{\epsilon_B + U} = P_w \frac{\epsilon_w - 1}{\epsilon_w + U} + P_i \frac{\epsilon_i - 1}{\epsilon_i + U} + P_a \frac{\epsilon_a - 1}{\epsilon_a + U} \qquad (9)$$

where ϵ_B, ϵ_w, ϵ_i, and ϵ_a are the dielectric constant of BB particle, water, ice, and air, respectively, P_w, P_i, and P_a are the volume content of water, ice, and air. respectively, and U is the form factor. Since ϵ_a is very close to 1.0 so that the last term in the right side of (9) can be ignored. We compute ϵ_w by using the Debye formula with parameters given in [10] and ϵ_i by using the formula in [11] for the real part, and the formula in [12] (or in [13]) for the imaginary part.

The quantity P_w is given by (5) and P_i can be shown to be given by

$$P_i = (\rho_B - P_w)/\rho_i \qquad (10)$$

where ρ_i is the density of ice (=0.917 [g/cm^3]).

The form factor U is assumed to be computed from ρ_B by the following expression, which is obtained by fitting the tabulated values of U in [7]:

$$U = \begin{cases} 2.0 & \text{for } \rho_B \le 0.09 \\ 2.0e^{13.0(\rho_a - 0.09)} & \text{for } \rho_B > 0.09 \end{cases} \qquad (11)$$

The above (11) also can be used for obtaining U in the upper snow region when ρ_B is replaced with the density of a snowflake ρ_s.

With these preparations, we can now go on to describe the essence of our new approach. But before doing that, we will briefly explain the test data (see Fig. 1).

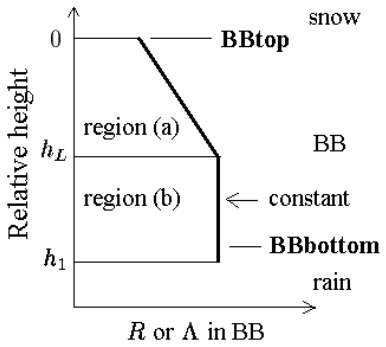

Fig. 2: Several heights in BB

Fig. 1 shows a height profile of the radar reflectivity factor Z which is obtained by averaging a one month amount of TRMM Precipitation Radar (PR) data. We use the version 6 TRMM PR data. The figure is obtained by using the PR data in the nadir direction only. All the data both over land and over ocean are used. The averaging is made by adjusting each peak value of Z in the BB profile to appear at the same relative height. The TRMM PR [1] has a range resolution of 250 m, but Fig. 1 is obtained by using the over-sampled data with a 125 m interval. The footprint size of the TRMM PR antenna beam is about 4.3 km in diameter. The frequency of the TRMM PR is 13.8 GHz.

We need to determine the upper boundary of bright band, BBtop, where the melting of snowflakes starts. Numerical results indicate that the value of Z at the BBtop should be smaller than the value of Z at the rain top, otherwise the model would predict a strange and unacceptable Z profile of BB. From a practical point of view, we assume that the height of BBtop in Fig.1 is 375 m (i.e., 125×3 m) higher than the height of BB peak.

In our approach, two quantities in BB, that is the precipitation rate R_B and the DSD slope Λ_B, are connected from snow region to the rain region in linear functional forms with respect to the height (see Fig. 2).

In Fig.2, two heights h_L and h_1 are introduced below BBtop. From BBtop down to the height h_L, i.e, in the region (a), the above mentioned linear interpolations are made. Note that the height h_L is located inside the BB, but h_1 is located in the rain region. The height h_1 should belong to rain region but should be close to the lower boundary of BB, BBbottom. (We will not discuss BBbottom, whose definition is different for authors [14][15]). From a practical reason, we choose the height h_1 to be located at 1000 m below BBtop. In the region (b) in Fig. 2, precipitation rate and DSD slope are constant and they are equal to R_1 at h_1 and Λ_1 at h_1, respectively.

Let us denote the precipitation rate and the slope of DSD at BBtop as R_{s0} and Λ_{s0}, respectively. Let us also denote these two quantities at the relative height h_L as R_L and Λ_L, respectively,

In the snow region, Eq. (3) holds so that either R_{s0} or Λ_{s0} is the only free variable.

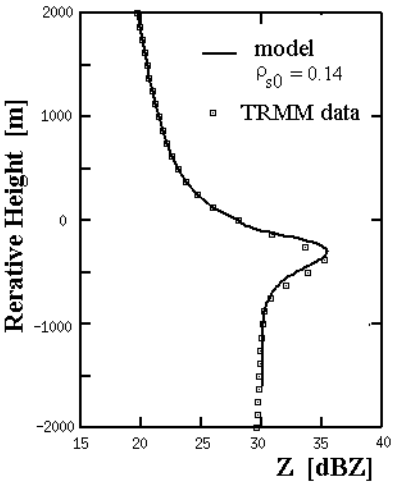

Fig. 3: Computed profile of Z (solid line)

In the rain region, we assume an exponential type DSD so that the following relation [16] holds for raindrops.

$$\Lambda \;=\; 41R^{-0.21} \quad [\mathrm{cm}^{-1}] \tag{12}$$

Because of (12), either R or Λ is the only free variable in the rain region.

In the region (b) in Fig.2, the precipitation rate and DSD slope are assumed to be constant so that (12) also holds when R is replaced with R_L and Λ with Λ_L.

In the region (a) in Fig.2, however, there does not exists any pre-determined relation between R and Λ: we can assign both R and Λ in the region (a).

We need to determine the height h_L which separates regions (a) and (b). We assume that h_L [m] is given by the following formula

$$h_L \;=\; -100Z_1^{0.17} - 100 \tag{13}$$

where Z_1 [mm^{6}m^{-3}] is the reflectivity factor at h_1. When Z_1 is replaced with Z at BBbottom, Z_R, the first term on the right side of (13) becomes the BB width given by Klaassen [14] (times a minus sign). We assume here that Z_R would be very close to Z_1. A 100m offset is introduced in (13) because Klaassen's BB width is thought to be too narrow [15].

Since the observed Z in Fig. 1 contains the attenuation, the observed Z at h_1 is not Z_1. We compute Z_1 in the following iteration.

From the observed Z at h_1, Z_{1m}, we obtain the first guess of R, R_{1st}, by the following relation [16]

$$Z_{1m} \;=\; 200R_{1st}^{1.6} \tag{14}$$

Run the program with this initial guess value, and obtain the computed value of Z_{1est}. Make a correction to R_{1st} using Z_{1est}/Z_{1m}. Though this process can be repeated, making a correction only once seems to be sufficient.

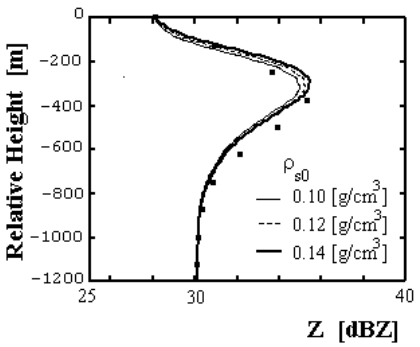

Fig. 4: Dependence of computed Z on ρ_{s0}

3. RESULTS

Fig. 3 shows the model result (solid line) which is compared with the observed averaged data of TRMM PR at 13.8 GHz; the data points here are the same as those shown in Fig. 1. We run the model with several ρ_{s0}, which is the density of snow at BBtop. Fig. 3 shows the case for $\rho_{s0} = 0.14$ [g/cm^3].

Fig. 4 shows Z in BB calculated for different ρ_{s0} together with observed data points. Among the three curves, the one for $\rho_{s0} = 0.14$ seems to fit the data best.

In the snow region, attenuation due to snow is ignored so that the modeled Z is the same as the observed data. In other words, we trust observed Z of snow and calculate R and Λ of snow (see Figs. 5 and 6). In this calculation, the density of snow is assumed to be constant in height and is equal to ρ_{s0}.

A detailed examination of Fig. 3 shows that there exists a small gap in the slope of Z at BBtop. Fig. 4 shows that about a 100 m difference exists between the height of computed BB peak and that of measured peak. On the whole, however, it may be said that our model can produce a reasonable value of Z in BB.

Fig. 5 shows computed profile of precipitation rate R. The figure indicates that R shows only a gradual downward increase at higher altitude but the increase of R becomes appreciable as the height decreases. It should be noted that a very rapid downward increase of R already begins above BBtop. The downward increase of R continues in the upper part of BB until the height reaches to h_L (by our assumption R changes linearly with respect to height from BBtop down to h_L).

Fig. 6 shows computed profile of Λ. In the higher altitude, Λ shows a large value, which means that small drops are dominant in the upper snow region. The slope Λ decreases as the height decreases which implies a formation of large drops as the snowflakes fall. The slope Λ reaches to the minimum value at BBtop, implying that the formation of large drops may occur most intensely at BBtop. From BBtop down to h_L, Λ increases (linearly with height by the assumption).

4. DISCUSSIONS

The most interesting finding of this study would be the fact that the precipitation rate which is smaller than the value

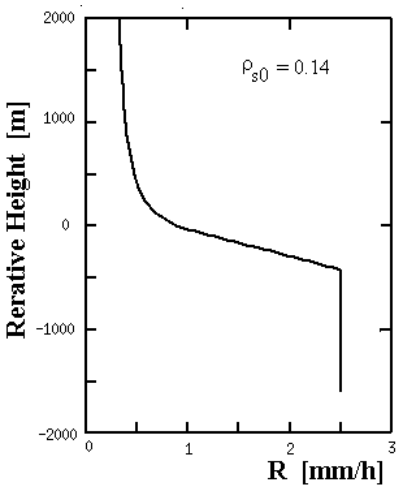

Fig. 5: Computed profile of R

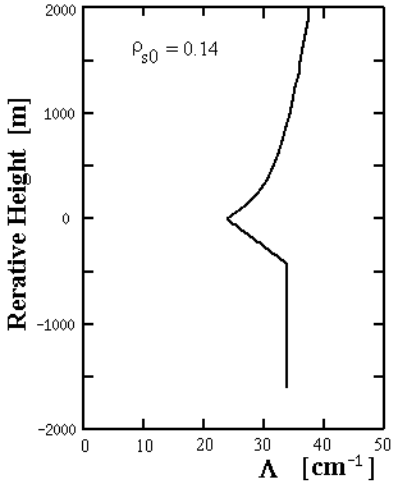

Fig. 6: Computed profile of Λ

at BBbottom can produce the BB peak in Z; this fact is obtained by comparing Figs. 3, 5, and 6. The maximum value of Z, Z_{peak}, appear about a 100 m above h_t. The precipitation rate at the height where Z_{peak} appears is smaller than the precipitation rate at h_t, hence smaller than the value at BBbottom.

Below h_t, Z shows a value larger than that of rain because melting of larger drops does not end at h_t, so that the actual size of a melting drop is larger than the melted size, and the fall velocity is smaller than that of a melted drop (see (4) on the effect of velocity on DSD). Contribution of such still melting drops causes the tailing part of BB peak.

A care should be taken on the fact, however, that TRMM PR has a 250 m range resolution so that the observed Z is a range averaged quantity. If the range average were not made, the actual peak value of Z would be slightly larger than the observed one and the width of the peak would be slightly narrower than the observed one.

5. CONCLUSIONS

We have developed a BB model in which the precipitation rate is changed from a small value in the upper snow region to a larger value in the rain region in a reasonable way. The model can successfully explain the averaged profile of Z observed by the TRMM PR. However, there are rooms for possible improvement in the model, such as in the choice of parameters, inclusion of the reported dependence of ρ_s on the drop size [9][14] into the model, and also in the selection of composite dielectric model. Further works are necessary. Application of the model to other experimental data with different frequencies and comparison with Doppler data is also important.

ACKNOWLEDGMENTS

This study has been funded by Japan Aerospace Exploration Agency (JAXA) under TRMM program and also by Japan Science and Technology Agency (JST) under CREST program.

REFERENCES

[1] T. Iguchi, T.Kozu, R. Meneghini, J. Awaka, K. Okamoto, "Rain-Profiling Algorithm for the TRMM Precipitation Radar", *J. Appl. Meteor.*, Vol.39, No.12, 2000, pp. 2038-2052.

[2] K.L.S. Gunn, J.S. Marshall, "The distribution with size of aggregate snowflakes", *J. Meteor.*, Vol.15, No.2, 1958, pp. 452-461.

[3] R.S. Sekhon, R.C. Srivastava, "Snow size spectra and radar reflectivity", *J. Atmos. Sci.*, Vol.27, No.2, 1970, pp. 209-307.

[4] T. Yokoyama, H. Tanaka, "Microphysical processes of melting snowflakes detected by two-wavelength radar Part I. Principle of measurement based on model calculation", *J. Meteor. Soc. Japan*, Vol.62, No.4, 1984, pp. 650-666.

[5] G.B. Foote, P.S. Du Toit, "Terminal velocity of raindrops aloft", *J. Appl. Meteor.*, Vol.8, 1969, pp. 249-253.

[6] A. Nishitsuji, "Method of calculation of radio-wave attenuation in snowfall", *Trans. IEICE Japan*, Vol. 54-B, No.1, 1971, pp. 611-618 (in Japanese).

[7] J. Awaka, Y. Furuhama, M. Hoshiyama, A. Nishitsuji, "Model calculations of scattering properties of spherical bright-band particles made of composite dielectrics", *J. Radio. Res. Lab.*, Vol. 32, No. 136, 1985, pp. 73-87.

[8] M. Thurai, H. Kumagai, T. Kozu, J. Awaka, "Effects of incorporating a brightband model in a downward-looking radar rainfall retrieval Algorithm", *J. Atmos. Oceanic Tec.*, Vol. 18, No. 1, 2001, pp. 20-25.

[9] P. Bauer, A. Khain, A. Pokrovsky, R. Meneghini, C. Kummerow, F. Marzano, J.P.V. Poiares Baptista, "Combined cloud-microwave radiative transfer modeling of stratiform rainfall", *J. Atmos. Sci.*, Vol. 57, No. 8, 2000, pp. [1082-1104].

[10] F.T. Ulaby, R.K. Moore, A.K. Fung, *Microwave Remote Sensing*, Vol.III, Artec House, 1986.

[11] C. Mätzler, U. Wegmüller, "Dielectric properties of fresh-water ice at microwave frequencies", *J. Phys. D: Appl. Phys.Proc.*, Vol. 20, 1987, pp. 1623-1630.

[12] A. Wiesmann, C. Mätzler, T. Weise, "Radiometric and structural measurements of snow samples", *Radio Science*, Vol.33, 1998, pp. 273-289.

[13] G. Hufford, "A model for the complex permittivity of ice at frequencies below 1 THz", *Int. J. Infrared Millimeter Waves*, Vol. 12, 1991, pp. 677-682.

[14] Klaassen, "Radar observations and simulation of the melting layer of precipitation", *aJ. Atmos. Sci.*, Vol. 45, pp. 3741-3753.

[15] F. Fabry, I. Zawadzki, "Long-term radar observations of the melting layer of precipitation and their interpretation", *J. Atmos. Sci.*, Vol. 52, pp. 838-851.

[16] J.S. Marshall, W.M. Palmer, "The distribution of raindrops with size", *J. Meteor.*, Vol. 5, 1948, pp. 165-166.